



# The International Association for the Properties of Water and Steam

Prague, Czech Republic  
September 2018

## Revised Release on the IAPWS Formulation 2017 for the Thermodynamic Properties of Heavy Water

©2018 International Association for the Properties of Water and Steam  
Publication in whole or in part is allowed in all countries provided that attribution is given to the  
International Association for the Properties of Water and Steam

Please cite as: International Association for the Properties of Water and Steam, IAPWS R16-17(2018),  
*Revised Release on the IAPWS Formulation 2017 for the Thermodynamic Properties of Heavy Water* (2018)

This revised release replaces the corresponding release of 2017, which replaced the revised release of  
2005 (IAPWS R3-84(2005)), and contains 17 pages, including this cover page.

This Revised Release has been authorized by the International Association for the Properties of Water and Steam (IAPWS) at its meeting in Prague, Czech Republic, 2-7 September, 2018. The members of IAPWS are: Australia, Britain and Ireland, Canada, the Czech Republic, Germany, Japan, New Zealand, Russia, Scandinavia (Denmark, Finland, Norway, Sweden), and the United States, and associate members Argentina and Brazil, China, Egypt, France, Greece, Italy, and Switzerland. The President at the time of adoption of this document was Prof. Hans-Joachim Kretzschmar of Germany.

### Summary

The formulation provided in this Release is recommended for calculating thermodynamic properties of heavy water, which IAPWS defines as water whose hydrogen atoms are entirely the deuterium isotope ( $^2\text{H}$  or  $\text{D}$ ) and whose oxygen atoms have the isotopic composition of ordinary water [1]. Further details about the formulation can be found in the article “A Reference Equation of State for Heavy Water” by S. Herrig *et al.* [2]. This formulation provides the most accurate representation available at the time this Release was prepared for the thermodynamic properties of the fluid phases of heavy water over a wide range of conditions.

A revision to the original 2017 Release was adopted in 2018 in order to reduce the uncertainty for properties (particularly density) in the liquid region.

Further information about this Revised Release and other documents issued by IAPWS can be obtained from the Executive Secretary of IAPWS (Dr. R.B. Dooley, [bdooley@iapws.org](mailto:bdooley@iapws.org)) or from <http://www.iapws.org>.

## Contents

1	Nomenclature	2
2	Reference Constants	3
3	The Formulation	3
4	Relations of Thermodynamic Properties to the Dimensionless Helmholtz Free Energy	5
5	Range of Validity	9
6	Melting and Sublimation Curves	10
7	Estimates of Uncertainty	11
8	Computer-Program Verification	11
9	References	13

## 1 Nomenclature

### *Thermodynamic quantities:*

$B$	Second virial coefficient
$C$	Third virial coefficient
$c_p$	Molar isobaric heat capacity
$c_v$	Molar isochoric heat capacity
$f$	Molar Helmholtz free energy
$h$	Molar enthalpy
$M$	Molar mass
$p$	Pressure
$R$	Molar gas constant
$s$	Molar entropy
$T$	Absolute temperature
$u$	Molar internal energy
$w$	Speed of sound
$\alpha$	Dimensionless Helmholtz free energy, $\alpha = f/(RT)$
$\beta_s$	Isentropic throttling coefficient
$\delta$	Reduced density, $\delta = \rho/\rho_c$
$\delta_T$	Isothermal throttling coefficient
$\kappa_T$	Isothermal compressibility
$\mu$	Joule-Thomson coefficient
$\theta$	Reduced temperature, $\theta = T/T_n$
$\rho$	Molar density
$\tau$	Inverse reduced temperature, $\tau = T_c/T$

### *Superscripts*

o	ideal-gas property
r	residual
'	saturated liquid state
"	saturated vapor state

### *Subscripts*

c	critical point
m	melting
n	reducing parameter
subl	sublimation
t	triple point
$\sigma$	vapor-liquid saturation

Note:  $T$  denotes absolute temperature on the International Temperature Scale of 1990. This is unaffected by the revision to the SI system of units scheduled to go into effect in 2019.

## 2 Reference Constants

$$T_c = 643.847 \text{ K} \quad (1)$$

$$\rho_c = 17.775 \text{ 55 mol dm}^{-3} \quad (2)$$

$$R = 8.314 \text{ 459 8 J mol}^{-1} \text{ K}^{-1} \quad (3)$$

$$M = 20.027 \text{ 508 g mol}^{-1} \quad (4)$$

The numerical value for the critical temperature  $T_c$  is identical to that given in the IAPWS release on the critical parameters of ordinary and heavy water [3]. The value for the critical density  $\rho_c$  is the massic critical density given in [3] converted to molar density by the molar mass  $M$ , which is that given in [1]. The value of the molar gas constant  $R$  is that given by the 2014 CODATA evaluation [4].

Due to the use of the molar gas constant, Eq. (5) corresponds to a mole-based formulation. In order to convert values of molar properties to mass-based properties, a molar mass must be used. In general, this should be the value of  $M$  given by Eq. (4). In some special cases (such as heavy water that is enriched in heavy oxygen isotopes), specific information may be available that the isotopic composition differs from the definition of heavy water given in [1]; in such cases it may be appropriate to use a different molar mass corresponding to that different isotopic composition.

## 3 The Formulation

The formulation is a fundamental equation for the molar Helmholtz free energy  $f$ . This equation is expressed in dimensionless form,  $\alpha = f/(RT)$ , and is separated into two parts, an ideal-gas part  $\alpha^\circ$  and a residual part  $\alpha^r$ , so that:

$$\frac{f(T, \rho)}{RT} = \alpha(\tau, \delta) = \alpha^\circ(\tau, \delta) + \alpha^r(\tau, \delta), \quad (5)$$

where  $\tau = T_c/T$  and  $\delta = \rho/\rho_c$  with  $T_c$ ,  $\rho_c$ , and  $R$  given by Eqs. (1), (2), and (3).

The ideal-gas part  $\alpha^\circ$  of the dimensionless Helmholtz free energy is obtained from a fit to the high-accuracy calculations by Simkó *et al.* [5] of the isobaric heat capacity in the ideal-gas state. It is given by:

$$\alpha^\circ(\tau, \delta) = a_1 + a_2\tau + \ln \delta + (c_0 - 1) \ln \tau + \sum_{i=1}^4 v_i \ln [1 - \exp(-u_i \tau/T_c)]. \quad (6)$$

Table 1 contains the coefficients and parameters of Eq. (6).

**Table 1.** Numerical values of the coefficients and parameters of the ideal-gas part of the dimensionless Helmholtz free energy, Eq. (6)

Parameter	Value	Parameter	Value
$c_0$	4.0		
$a_1$	-8.670 994 022 646 00		
$a_2$	6.960 335 784 587 78		
$v_1$	$0.106\ 33 \times 10^{-1}$	$u_1$	308 K
$v_2$	0.997 87	$u_2$	1695 K
$v_3$	$0.214\ 83 \times 10^1$	$u_3$	3949 K
$v_4$	0.354 9	$u_4$	10317 K

The form of the residual part  $\alpha^r$  of the dimensionless Helmholtz free energy is:

$$\alpha^r(\delta, \tau) = \sum_{i=1}^6 n_i \delta^{d_i} \tau^{t_i} + \sum_{i=7}^{12} n_i \delta^{d_i} \tau^{t_i} \exp(-\delta^{l_i}) + \sum_{i=13}^{24} n_i \delta^{d_i} \tau^{t_i} \exp\left[-\eta_i (\delta - \varepsilon_i)^2 - \beta_i (\tau - \gamma_i)^2\right]. \quad (7)$$

All parameters (coefficients  $n_i$ , temperature exponents  $t_i$ , density exponents  $d_i$  and  $l_i$ , and parameters of the Gaussian bell-shaped terms  $\eta_i$ ,  $\varepsilon_i$ ,  $\beta_i$ , and  $\gamma_i$ ) are listed in Table 2.

The IAPWS reference-state convention is that the internal energy and the entropy of the saturated liquid at the triple point are set equal to zero. Thus, at the triple-point temperature  $T_t = 276.969$  K [6],

$$u'_t = 0, \quad s'_t = 0. \quad (8)$$

In order to meet this condition, the coefficients  $a_1$  and  $a_2$  in Eq. (6) have been adjusted accordingly. Because of differences in computer codes (such as convergence tolerances), a particular computer code may produce values that differ slightly from the zeros in Eq. (8). If a user wants to reproduce Eq. (8) more precisely, the constants  $a_1$  and  $a_2$  in Eq. (6) may be readjusted by imposing the condition  $u'_t = 0, s'_t = 0$  with the desired accuracy.

**Table 2.** Numerical values of the coefficients and parameters of the residual part of the dimensionless Helmholtz free energy, Eq. (7)

$i$	$n_i$	$t_i$	$d_i$	$l_i$	$\eta_i$	$\beta_i$	$\gamma_i$	$\varepsilon_i$
1	$0.122\ 082\ 060 \times 10^{-1}$	1.0000	4	-				
2	$0.296\ 956\ 870 \times 10^1$	0.6555	1	-				
3	$-0.379\ 004\ 540 \times 10^1$	0.9369	1	-				
4	0.941 089 600	0.5610	2	-				
5	-0.922 466 250	0.7017	2	-				
6	$-0.139\ 604\ 190 \times 10^{-1}$	1.0672	3	-				
7	-0.125 203 570	3.9515	1	1				
8	$-0.555\ 391\ 500 \times 10^1$	4.6000	1	2				
9	$-0.493\ 009\ 740 \times 10^1$	5.1590	3	2				
10	$-0.359\ 470\ 240 \times 10^{-1}$	0.2000	2	1				
11	$-0.936\ 172\ 870 \times 10^1$	5.4644	2	2				
12	-0.691 835 150	2.3660	1	2				
13	$-0.456\ 110\ 600 \times 10^{-1}$	3.4553	1	-	0.6014	0.4200	1.5414	1.8663
14	$-0.224\ 513\ 300 \times 10^1$	1.4150	3	-	1.4723	2.4318	1.3794	0.2895
15	$0.860\ 006\ 070 \times 10^1$	1.5745	1	-	1.5305	1.2888	1.7385	0.5803
16	$-0.248\ 410\ 420 \times 10^1$	3.4540	3	-	2.4297	8.2710	1.3045	0.2236
17	$0.164\ 476\ 900 \times 10^2$	3.8106	1	-	1.3086	0.3673	2.7242	0.6815
18	$0.270\ 393\ 360 \times 10^1$	4.8950	1	-	1.3528	0.9504	3.5321	0.9495
19	$0.375\ 637\ 470 \times 10^2$	1.4300	2	-	3.4456	7.8318	2.4552	1.1158
20	$-0.177\ 607\ 760 \times 10^1$	1.5870	2	-	1.2645	3.3281	0.8319	0.1607
21	$0.220\ 924\ 640 \times 10^1$	3.7900	2	-	2.5547	7.1753	1.3500	0.4144
22	$0.519\ 652\ 000 \times 10^1$	2.6200	1	-	1.2148	0.9465	2.5617	0.9683
23	0.421 097 400	1.9000	1	-	18.738	1177.0	1.0491	0.9488
24	-0.391 921 100	4.3200	1	-	18.677	1167.0	1.0486	0.9487

#### 4 Relations of Thermodynamic Properties to the Dimensionless Helmholtz Free Energy

All thermodynamic properties can be derived from Eq. (5) by using the appropriate combinations of the ideal-gas part  $\alpha^\circ$ , Eq. (6), and the residual part  $\alpha^r$ , Eq. (7), of the dimensionless Helmholtz free energy and their derivatives. Relations between thermodynamic properties and  $\alpha^\circ$  and  $\alpha^r$  and their derivatives are summarized in Table 3. All required derivatives of the ideal-gas part and of the residual part of the Helmholtz free energy are given in Table 4 and Table 5, respectively.

Besides the single-phase region, the formulation also describes vapor-liquid equilibria. For a given temperature  $T$ , solving the phase-equilibrium equations (see Table 3) yields the saturation properties  $p_\sigma$ ,  $\rho'$ , and  $\rho''$  at  $T$ . With these, all other saturation properties can be derived from Eq. (5). In this way, the properties calculated on the saturation curve are thermodynamically consistent with the properties of the single-phase region.

**Table 3.** Relations of thermodynamic properties to the ideal-gas part  $\alpha^0$  and the residual part  $\alpha^r$  of the dimensionless Helmholtz free energy and their derivatives<sup>a</sup>

Property	Relation
Pressure $p = \rho^2 (\partial f / \partial \rho)_T$	$\frac{p(\delta, \tau)}{\rho RT} = 1 + \delta \alpha_\delta^r$
Molar internal energy $u = f - T(\partial f / \partial T)_\rho$	$\frac{u(\delta, \tau)}{RT} = \tau (\alpha_\tau^0 + \alpha_\tau^r)$
Molar entropy $s = -(\partial f / \partial T)_\rho$	$\frac{s(\delta, \tau)}{R} = \tau (\alpha_\tau^0 + \alpha_\tau^r) - \alpha^0 - \alpha^r$
Molar enthalpy $h = f - T(\partial f / \partial T)_\rho + \rho(\partial f / \partial \rho)_T$	$\frac{h(\delta, \tau)}{RT} = 1 + \tau (\alpha_\tau^0 + \alpha_\tau^r) + \delta \alpha_\delta^r$
Molar isochoric heat capacity $c_v = (\partial u / \partial T)_\rho$	$\frac{c_v(\delta, \tau)}{R} = -\tau^2 (\alpha_{\tau\tau}^0 + \alpha_{\tau\tau}^r)$
Molar isobaric heat capacity $c_p = (\partial h / \partial T)_p$	$\frac{c_p(\delta, \tau)}{R} = -\tau^2 (\alpha_{\tau\tau}^0 + \alpha_{\tau\tau}^r) + \frac{(1 + \delta \alpha_\delta^r - \delta \tau \alpha_{\delta\tau}^r)^2}{1 + 2\delta \alpha_\delta^r + \delta^2 \alpha_{\delta\delta}^r}$
Speed of sound $w = M^{-1/2} (\partial p / \partial \rho)_s^{1/2}$	$\frac{w^2(\delta, \tau)}{(RT/M)} = 1 + 2\delta \alpha_\delta^r + \delta^2 \alpha_{\delta\delta}^r - \frac{(1 + \delta \alpha_\delta^r - \delta \tau \alpha_{\delta\tau}^r)^2}{\tau^2 (\alpha_{\tau\tau}^0 + \alpha_{\tau\tau}^r)}$
Joule-Thomson coefficient $\mu = (\partial T / \partial p)_h$	$\mu R \rho = \frac{-(\delta \alpha_\delta^r + \delta^2 \alpha_{\delta\delta}^r + \delta \tau \alpha_{\delta\tau}^r)}{(1 + \delta \alpha_\delta^r - \delta \tau \alpha_{\delta\tau}^r)^2 - \tau^2 (\alpha_{\tau\tau}^0 + \alpha_{\tau\tau}^r) (1 + 2\delta \alpha_\delta^r + \delta^2 \alpha_{\delta\delta}^r)}$
Isothermal throttling coefficient $\delta_T \rho = (\partial h / \partial p)_T$	$\delta_T \rho = 1 - \frac{1 + \delta \alpha_\delta^r - \delta \tau \alpha_{\delta\tau}^r}{1 + 2\delta \alpha_\delta^r + \delta^2 \alpha_{\delta\delta}^r}$
Isentropic temperature-pressure coefficient $\beta_s = (\partial T / \partial p)_s$	$\beta_s \rho R = \frac{1 + \delta \alpha_\delta^r - \delta \tau \alpha_{\delta\tau}^r}{(1 + \delta \alpha_\delta^r - \delta \tau \alpha_{\delta\tau}^r)^2 - \tau^2 (\alpha_{\tau\tau}^0 + \alpha_{\tau\tau}^r) (1 + 2\delta \alpha_\delta^r + \delta^2 \alpha_{\delta\delta}^r)}$
Second virial coefficient $B(T) = \lim_{\rho \rightarrow 0} (\partial(p/(\rho RT)) / \partial \rho)_T$	$B(\tau) \rho_c = \lim_{\delta \rightarrow 0} \alpha_\delta^r(\delta, \tau) = \sum_{i=2,3,7,8,12} n_i \tau^{f_i} + \sum_{i=13,15,17,18,22,23,24} n_i \tau^{f_i} \exp[-\eta_i \varepsilon_i^2 - \beta_i (\tau - \gamma_i)^2]$
Third virial coefficient $C(T) = \lim_{\rho \rightarrow 0} \left[ \frac{1}{2} (\partial^2(p/(\rho RT)) / \partial \rho^2)_T \right]$	$C(\tau) \rho_c^2 = \lim_{\delta \rightarrow 0} \alpha_{\delta\delta}^r(\delta, \tau) = 2 \sum_{i=4,5,10,11} n_i \tau^{f_i} - 2n_7 \tau^{f_7} + 2 \sum_{i=19,20,21} n_i \tau^{f_i} \exp[-\eta_i \varepsilon_i^2 - \beta_i (\tau - \gamma_i)^2] + 4 \sum_{i=13,15,17,18,22,23,24} \varepsilon_i \eta_i n_i \tau^{f_i} \exp[-\eta_i \varepsilon_i^2 - \beta_i (\tau - \gamma_i)^2]$
Phase-equilibrium condition (Maxwell criterion)	$\frac{P\sigma}{RT\rho'} = 1 + \delta' \alpha_\delta^r(\delta', \tau) \quad ; \quad \frac{P\sigma}{RT\rho''} = 1 + \delta'' \alpha_\delta^r(\delta'', \tau)$ $\frac{P\sigma}{RT} \left( \frac{1}{\rho''} - \frac{1}{\rho'} \right) - \ln \left( \frac{\rho'}{\rho''} \right) = \alpha^r(\delta', \tau) - \alpha^r(\delta'', \tau)$

<sup>a</sup>  $\alpha_\delta^r = \left[ \frac{\partial \alpha^r}{\partial \delta} \right]_\tau$ ,  $\alpha_{\delta\delta}^r = \left[ \frac{\partial^2 \alpha^r}{\partial \delta^2} \right]_\tau$ ,  $\alpha_\tau^r = \left[ \frac{\partial \alpha^r}{\partial \tau} \right]_\delta$ ,  $\alpha_{\tau\tau}^r = \left[ \frac{\partial^2 \alpha^r}{\partial \tau^2} \right]_\delta$ ,  $\alpha_{\delta\tau}^r = \left[ \frac{\partial^2 \alpha^r}{\partial \delta \partial \tau} \right]$ ,  $\alpha_\tau^0 = \left[ \frac{\partial \alpha^0}{\partial \tau} \right]_\delta$ ,  $\alpha_{\tau\tau}^0 = \left[ \frac{\partial^2 \alpha^0}{\partial \tau^2} \right]_\delta$ .

**Table 4.** The ideal-gas part  $\alpha^o$  of the dimensionless Helmholtz free energy and its derivatives<sup>a</sup>


---



---

$\alpha^o$	=	$\ln\delta$	+	$a_1$	+	$a_2\tau$	+	$(c_o - 1)\ln\tau$	+	$\sum_{i=1}^4 v_i \ln\left[1 - e^{-(u_i\tau)/T_c}\right]$
$\alpha_{\delta}^o$	=	$1/\delta$	+	$0$	+	$0$	+	$0$	+	$0$
$\alpha_{\delta\delta}^o$	=	$-1/\delta^2$	+	$0$	+	$0$	+	$0$	+	$0$
$\alpha_{\tau}^o$	=	$0$	+	$0$	+	$a_2$	+	$(c_o - 1)/\tau$	+	$\sum_{i=1}^4 v_i u_i/T_c \left[ \frac{1}{1 - e^{-(u_i\tau)/T_c}} - 1 \right]$
$\alpha_{\tau\tau}^o$	=	$0$	+	$0$	+	$0$	-	$(c_o - 1)/\tau^2$	-	$\sum_{i=1}^4 v_i (u_i/T_c)^2 \frac{e^{-(u_i\tau)/T_c}}{\left[1 - e^{-(u_i\tau)/T_c}\right]^2}$
$\alpha_{\delta\tau}^o$	=	$0$	+	$0$	+	$0$	+	$0$	+	$0$

---

<sup>a</sup>  $\alpha_{\delta}^o = \left[ \frac{\partial \alpha^o}{\partial \delta} \right]_{\tau}$ ,  $\alpha_{\delta\delta}^o = \left[ \frac{\partial^2 \alpha^o}{\partial \delta^2} \right]_{\tau}$ ,  $\alpha_{\tau}^o = \left[ \frac{\partial \alpha^o}{\partial \tau} \right]_{\delta}$ ,  $\alpha_{\tau\tau}^o = \left[ \frac{\partial^2 \alpha^o}{\partial \tau^2} \right]_{\delta}$ ,  $\alpha_{\delta\tau}^o = \left[ \frac{\partial^2 \alpha^o}{\partial \delta \partial \tau} \right]$ .

**Table 5.** The residual part  $\alpha^r$  of the dimensionless Helmholtz free energy and its derivatives<sup>a</sup>

$$\alpha^r = \sum_{i=1}^6 n_i \delta^{d_i} \tau^{t_i} + \sum_{i=7}^{12} n_i \delta^{d_i} \tau^{t_i} e^{-\delta^{l_i}} + \sum_{i=13}^{24} n_i \delta^{d_i} \tau^{t_i} e^{-\eta_i(\delta-\varepsilon_i)^2 - \beta_i(\tau-\gamma_i)^2}$$

$$\alpha_{\delta}^r = \sum_{i=1}^6 n_i d_i \delta^{d_i-1} \tau^{t_i} + \sum_{i=7}^{12} n_i \delta^{d_i-1} \tau^{t_i} (d_i - l_i \delta^{l_i}) e^{-\delta^{l_i}} + \sum_{i=13}^{24} n_i \delta^{d_i-1} \tau^{t_i} e^{-\eta_i(\delta-\varepsilon_i)^2 - \beta_i(\tau-\gamma_i)^2} [d_i - 2\eta_i \delta (\delta - \varepsilon_i)]$$

$$\alpha_{\delta\delta}^r = \sum_{i=1}^6 n_i d_i (d_i - 1) \delta^{d_i-2} \tau^{t_i} + \sum_{i=7}^{12} n_i \delta^{d_i-2} \tau^{t_i} [(d_i - l_i \delta^{l_i})(d_i - 1 - l_i \delta^{l_i}) - l_i^2 \delta^{l_i}] e^{-\delta^{l_i}} + \sum_{i=13}^{24} n_i \tau^{t_i} e^{-\eta_i(\delta-\varepsilon_i)^2 - \beta_i(\tau-\gamma_i)^2} \cdot [-2\eta_i \delta^{d_i} + 4\eta_i^2 \delta^{d_i} (\delta - \varepsilon_i)^2 - 4d_i \eta_i \delta^{d_i-1} (\delta - \varepsilon_i) + d_i (d_i - 1) \delta^{d_i-2}]$$

$$\alpha_{\tau}^r = \sum_{i=1}^6 n_i t_i \delta^{d_i} \tau^{t_i-1} + \sum_{i=7}^{12} n_i t_i \delta^{d_i} \tau^{t_i-1} e^{-\delta^{l_i}} + \sum_{i=13}^{24} n_i \delta^{d_i} \tau^{t_i} e^{-\eta_i(\delta-\varepsilon_i)^2 - \beta_i(\tau-\gamma_i)^2} \left[ \frac{t_i}{\tau} - 2\beta_i (\tau - \gamma_i) \right]$$

$$\alpha_{\tau\tau}^r = \sum_{i=1}^6 n_i t_i (t_i - 1) \delta^{d_i} \tau^{t_i-2} + \sum_{i=7}^{12} n_i t_i (t_i - 1) \delta^{d_i} \tau^{t_i-2} e^{-\delta^{l_i}} + \sum_{i=13}^{24} n_i \delta^{d_i} \tau^{t_i} e^{-\eta_i(\delta-\varepsilon_i)^2 - \beta_i(\tau-\gamma_i)^2} \left[ \left( \frac{t_i}{\tau} - 2\beta_i (\tau - \gamma_i) \right)^2 - \frac{t_i}{\tau^2} - 2\beta_i \right]$$

$$\alpha_{\delta\tau}^r = \sum_{i=1}^6 n_i d_i t_i \delta^{d_i-1} \tau^{t_i-1} + \sum_{i=7}^{12} n_i t_i \delta^{d_i-1} \tau^{t_i-1} (d_i - l_i \delta^{l_i}) e^{-\delta^{l_i}} + \sum_{i=13}^{24} n_i \delta^{d_i} \tau^{t_i} e^{-\eta_i(\delta-\varepsilon_i)^2 - \beta_i(\tau-\gamma_i)^2} \left[ \frac{d_i}{\delta} - 2\eta_i (\delta - \varepsilon_i) \right] \left[ \frac{t_i}{\tau} - 2\beta_i (\tau - \gamma_i) \right]$$

---


$$^a \alpha_{\delta}^r = \left[ \frac{\partial \alpha^r}{\partial \delta} \right]_{\tau}, \alpha_{\delta\delta}^r = \left[ \frac{\partial^2 \alpha^r}{\partial \delta^2} \right]_{\tau}, \alpha_{\tau}^r = \left[ \frac{\partial \alpha^r}{\partial \tau} \right]_{\delta}, \alpha_{\tau\tau}^r = \left[ \frac{\partial^2 \alpha^r}{\partial \tau^2} \right]_{\delta}, \alpha_{\delta\tau}^r = \left[ \frac{\partial^2 \alpha^r}{\partial \delta \partial \tau} \right].$$

## 5 Range of Validity

IAPWS has tested the formulation and endorses its validity in the following way:

- (1) The formulation is valid in the entire stable fluid region of D<sub>2</sub>O from the melting-pressure curve (see Section 6) to 825 K at pressures from the triple-point pressure to 1200 MPa; the lowest temperature on the melting-pressure curve is 254.415 K (at 222.40 MPa). At pressures below the triple-point pressure and temperatures above 100 K, it is also valid for the stable vapor at temperatures from the sublimation curve<sup>1</sup> up to 825 K.

In this entire region, Eq. (5) represents the experimental data available at the time the Release was prepared (except for very few data points) to within their uncertainties.

Although Eq. (5) is also in satisfactory agreement with the limited experimental data in the critical region, the equation, like any analytical Helmholtz energy formulation, is not able to reproduce the nonclassical values of critical exponents in the immediate vicinity of the critical point.

- (2) In the stable fluid region, the formulation can also be extrapolated beyond the limits given under item (1). Tests show that Eq. (5) behaves reasonably when extrapolated to pressures up to about 100 GPa and temperatures up to about 5000 K. This holds at least for the density and enthalpy of undissociated D<sub>2</sub>O.
- (3) The formulation behaves reasonably when extrapolated into the metastable regions. Equation (5) is in general agreement, in most cases within experimental uncertainties, with the currently available experimental data of the subcooled liquid (metastable with respect to solid). No reliable experimental data are available for either the superheated liquid (metastable with respect to vapor) or the supercooled vapor (metastable with respect to liquid), but the behavior of Eq. (5) when extrapolated into these regions is physically reasonable.

For further details, see [2].

---

<sup>1</sup> Note that the equation for the sublimation curve in Section 6 should not be extrapolated below 150 K.

## 6 Melting and Sublimation Curves

While IAPWS has not made an official recommendation for the melting and sublimation curves of heavy water, it is necessary to have a representation of these curves in order to compute the boundaries of the range of validity as given in Section 5. For that purpose, the correlations given in [2] are adopted, and summarized here.

*Melting-pressure equation for D<sub>2</sub>O ice Ih* (temperature range from 276.969 K to 254.415 K):

$$\frac{P_{\text{m,ice Ih}}}{p_n} = 1 - 0.301\,53 \times 10^5 (1 - \theta^{5.5}) + 0.692\,503 \times 10^6 (1 - \theta^{8.2}), \quad (9)$$

with reduced temperature  $\theta = T/T_n$  and the reducing parameters  $T_n = 276.969$  K and  $p_n = 0.000\,661\,59$  MPa. For checking computer implementations, at 270 K Eq. (9) gives a melting pressure of  $0.837\,888\,413 \times 10^2$  MPa.

*Melting-pressure equation for D<sub>2</sub>O ice III* (temperature range from 254.415 K to 258.661 K):

$$\frac{P_{\text{m,ice III}}}{p_n} = 1 - 0.802\,871 \times 10^0 (1 - \theta^{33}), \quad (10)$$

with  $\theta = T/T_n$ ,  $T_n = 254.415$  K, and  $p_n = 222.41$  MPa. For checking computer implementations, at 255 K Eq. (10) gives a melting pressure of  $0.236\,470\,168 \times 10^3$  MPa.

*Melting-pressure equation for D<sub>2</sub>O ice V* (temperature range from 258.661 K to 275.748 K):

$$\frac{P_{\text{m,ice V}}}{p_n} = 1 - 0.128\,038\,8 \times 10^1 (1 - \theta^{7.6}), \quad (11)$$

with  $\theta = T/T_n$ ,  $T_n = 258.661$  K, and  $p_n = 352.19$  MPa. For checking computer implementations, at 275 K Eq. (11) gives a melting pressure of  $0.619\,526\,971 \times 10^3$  MPa.

*Melting-pressure equation for D<sub>2</sub>O ice VI* (temperature range from 275.748 K to 315 K):

$$\frac{P_{\text{m,ice VI}}}{p_n} = 1 - 0.127\,602\,6 \times 10^1 (1 - \theta^4), \quad (12)$$

with  $\theta = T/T_n$ ,  $T_n = 275.748$  K, and  $p_n = 634.53$  MPa. For checking computer implementations, at 300 K Eq. (12) gives a melting pressure of  $0.959\,203\,594 \times 10^3$  MPa.

*Sublimation-pressure equation for D<sub>2</sub>O ice Ih* (temperature range from 210 K to 276.969 K):

$$\ln\left(\frac{P_{\text{subl}}}{p_n}\right) = -0.131\,422\,6 \times 10^2 (1 - \theta^{-1.73}) + 0.321\,296\,9 \times 10^2 (1 - \theta^{-1.42}), \quad (13)$$

with  $\theta = T/T_n$ ,  $T_n = 276.969$  K, and  $p_n = 0.000\,661\,59$  MPa. For checking computer implementations, at 245 K Eq. (13) gives a sublimation pressure of  $0.327\,390\,934 \times 10^{-4}$  MPa. Equation (13) extrapolates reasonably down to at least 150 K.

## 7 Estimates of Uncertainty

Estimates have been made of the uncertainty of the density, speed of sound, isobaric heat capacity, and vapor-liquid saturation pressure and coexisting densities when calculated from the formulation, Eq. (5). These estimates were derived from comparisons with the various sets of experimental data together with the judgment of the Working Group on Thermophysical Properties of Water and Steam of IAPWS. IAPWS considers these as estimates of the expanded uncertainties with coverage factor  $k = 2$ , roughly corresponding to a 95 % confidence interval.

For the single-phase region, these values are indicated in Figs. 1–3, which give the estimated uncertainties in various regions. With regard to the uncertainty for the speed of sound and the specific isobaric heat capacity, see Figs. 2 and 3, it should be noted that the uncertainties for these properties increase drastically when approaching the critical point. The statement “no definitive uncertainty estimates possible” for some regions is based on the lack of experimental data in the region. However, because the formulation was validated against experimental data and with regard to correct physical behavior over its entire range of validity, the results in these regions should be physically reasonable.

As noted in the captions of Figs. 1–3, the uncertainties of properties for the vapor at low pressures become small. This is because the low-density vapor approaches the ideal-gas limit; the ideal-gas behavior is known essentially exactly for the density and to a relatively small uncertainty for the speed of sound and isobaric heat capacity.

For the saturation properties, the estimates of the expanded uncertainties of vapor pressure, saturated liquid density, and saturated vapor density are shown in Fig. 4.

## 8 Computer-Program Verification

To assist the user in computer-program verification, three tables with test values are given. Table 6 contains values of the ideal-gas part  $\alpha^\circ$  and the residual part  $\alpha^r$  of the dimensionless Helmholtz free energy together with the corresponding derivatives. Table 7 lists values for the pressure  $p$ , the specific isochoric heat capacity  $c_v$ , the speed of sound  $w$ , and the specific entropy  $s$  calculated at selected values of temperature  $T$  and density  $\rho$ . Table 8 gives values for the vapor pressure  $p_\sigma$ , values for the density  $\rho'$ , enthalpy  $h'$ , and entropy  $s'$  for the saturated liquid, and values for the density  $\rho''$ , enthalpy  $h''$ , and entropy  $s''$  for the saturated vapor. All these saturation values have been calculated with Eq. (5) by using the phase-equilibrium condition (see the corresponding comment in Section 4).

**Table 6.** Values for the ideal-gas part  $\alpha^o$ , Eq. (6), and for the residual part  $\alpha^r$ , Eq. (7), of the dimensionless Helmholtz free energy together with the corresponding derivatives<sup>a</sup> for  $T = 500$  K and  $\rho = 46.26$  mol dm<sup>-3</sup>

$\alpha^o = 0.196\ 352\ 717 \times 10^1$	$\alpha^r = -0.342\ 291\ 092 \times 10^1$
$\alpha_{\delta}^o = 0.384\ 253\ 134$	$\alpha_{\delta}^r = -0.367\ 562\ 780$
$\alpha_{\delta\delta}^o = -0.147\ 650\ 471$	$\alpha_{\delta\delta}^r = 0.835\ 183\ 806$
$\alpha_{\tau}^o = 0.939\ 259\ 413 \times 10^1$	$\alpha_{\tau}^r = -0.589\ 707\ 436 \times 10^1$
$\alpha_{\tau\tau}^o = -0.209\ 517\ 144 \times 10^1$	$\alpha_{\tau\tau}^r = -0.245\ 187\ 285 \times 10^1$
$\alpha_{\delta\tau}^o = 0$	$\alpha_{\delta\tau}^r = -0.113\ 178\ 440 \times 10^1$

<sup>a</sup> For the abbreviated notation of the derivatives of  $\alpha^o$  and  $\alpha^r$  see the footnotes of Tables 4 and 5, respectively.

**Table 7.** Thermodynamic property values in the single-phase region for selected values of  $T$  and  $\rho$

$T/\text{K}$	$\rho/(\text{mol dm}^{-3})$	$p/\text{MPa}$	$c_v/(\text{J mol}^{-1} \text{K}^{-1})$	$w/(\text{m s}^{-1})$	$s/(\text{J mol}^{-1} \text{K}^{-1})$
300	$0.551\ 26 \times 10^2$	$0.529\ 123\ 711 \times 10^{-1}$ <sup>a</sup>	$0.833\ 839\ 128 \times 10^2$	$0.140\ 374\ 625 \times 10^4$	$0.673\ 910\ 582 \times 10^1$
	$0.600\ 00 \times 10^2$	$0.238\ 222\ 326 \times 10^3$	$0.738\ 561\ 038 \times 10^2$	$0.177\ 279\ 674 \times 10^4$	$0.540\ 117\ 148 \times 10^1$
	$0.650\ 00 \times 10^2$	$0.626\ 176\ 781 \times 10^3$	$0.699\ 125\ 978 \times 10^2$	$0.229\ 697\ 942 \times 10^4$	$0.271\ 566\ 150 \times 10^1$
500	$0.500\ 00 \times 10^{-1}$	0.206 052 588	$0.294\ 298\ 102 \times 10^2$	$0.514\ 480\ 413 \times 10^3$	$0.140\ 879\ 085 \times 10^3$
	0.500 00	$0.188\ 967\ 446 \times 10^1$	$0.366\ 460\ 545 \times 10^2$	$0.489\ 633\ 254 \times 10^3$	$0.120\ 227\ 024 \times 10^3$
	$0.462\ 60 \times 10^2$	$0.835\ 329\ 492 \times 10^1$	$0.626\ 885\ 994 \times 10^2$	$0.117\ 888\ 631 \times 10^4$	$0.495\ 587\ 000 \times 10^2$
	$0.500\ 00 \times 10^2$	$0.107\ 462\ 884 \times 10^3$	$0.617\ 372\ 286 \times 10^2$	$0.148\ 374\ 868 \times 10^4$	$0.469\ 453\ 826 \times 10^2$
	$0.600\ 00 \times 10^2$	$0.721\ 798\ 322 \times 10^3$	$0.576\ 860\ 681 \times 10^2$	$0.241\ 393\ 520 \times 10^4$	$0.393\ 599\ 094 \times 10^2$
643.8	$0.200\ 00 \times 10^2$	$0.216\ 503\ 820 \times 10^2$	$0.992\ 661\ 842 \times 10^2$	$0.256\ 043\ 612 \times 10^3$	$0.817\ 656\ 125 \times 10^2$
800	$0.100\ 00 \times 10^{-1}$	$0.664\ 864\ 175 \times 10^{-1}$	$0.340\ 033\ 604 \times 10^2$	$0.642\ 794\ 634 \times 10^3$	$0.169\ 067\ 586 \times 10^3$
	0.250 00	$0.164\ 466\ 177 \times 10^1$	$0.344\ 327\ 932 \times 10^2$	$0.639\ 281\ 410 \times 10^3$	$0.142\ 125\ 615 \times 10^3$

<sup>a</sup> In the liquid-water region at low pressures, small changes in density along an isotherm cause large changes in pressure. For this reason, due to an accumulation of small errors, a particular computer code or a particular computer may fail to reproduce the pressure value with nine significant figures.

**Table 8.** Thermodynamic property values for vapor-liquid saturation states at selected temperatures<sup>a</sup>

	$T = 280 \text{ K}$	$T = 450 \text{ K}$	$T = 625 \text{ K}$
$p_{\sigma}/\text{MPa}$	$0.823\ 054\ 058 \times 10^{-3}$	0.921 212 105	$0.172\ 118\ 129 \times 10^2$
$\rho'/(\text{mol dm}^{-3})$	$0.552\ 072\ 786 \times 10^2$	$0.492\ 937\ 575 \times 10^2$	$0.306\ 770\ 554 \times 10^2$
$\rho''/(\text{mol dm}^{-3})$	$0.353\ 747\ 143 \times 10^{-3}$	0.264 075 691	$0.694\ 443\ 339 \times 10^1$
$h'/(\text{J mol}^{-1})$	$0.257\ 444\ 444 \times 10^3$	$0.145\ 127\ 149 \times 10^5$	$0.324\ 533\ 556 \times 10^5$
$h''/(\text{J mol}^{-1})$	$0.466\ 106\ 716 \times 10^5$	$0.515\ 019\ 146 \times 10^5$	$0.472\ 460\ 343 \times 10^5$
$s'/(\text{J mol}^{-1} \text{ K}^{-1})$	0.924 406 091	$0.406\ 584\ 121 \times 10^2$	$0.731\ 042\ 291 \times 10^2$
$s''/(\text{J mol}^{-1} \text{ K}^{-1})$	$0.166\ 471\ 646 \times 10^3$	$0.122\ 856\ 634 \times 10^3$	$0.967\ 725\ 149 \times 10^2$

<sup>a</sup> All these test values were calculated from the Helmholtz free energy, Eq. (5), by applying the phase-equilibrium condition (Maxwell criterion).

## 9 References

- [1] IAPWS, G5-01(2016), *Guideline on the Use of Fundamental Physical Constants and Basic Constants of Water* (2001). Available from <http://www.iapws.org>.
- [2] Herrig, S., Thol, M., Harvey, A.H., and Lemmon, E.W., A Reference Equation of State for Heavy Water, *J. Phys. Chem. Ref. Data* **47**, 043102 (2018).
- [3] IAPWS, R2-83(1992), *Release on the Values of Temperature, Pressure, and Density of Ordinary and Heavy Water Substances at Their Respective Critical Points* (1992). Available from <http://www.iapws.org>.
- [4] Mohr, P.J., Newell, D.B., and Taylor, B.N., CODATA Recommended Values of the Fundamental Physical Constants: 2014, *J. Phys. Chem. Ref. Data* **45**, 043102 (2016) [also published in *Rev. Mod. Phys.* **88**, 035009 (2016)].
- [5] Simkó, I., Furtenbacher, T., Hrubý, J., Zobov, N.F., Polyansky, O.L., Tennyson, J., Gamache, R.R., Szidarovszky, T., Dénes, N., and Császár, A.G., Recommended Ideal-gas Thermochemical Functions for Heavy Water and its Substituent Isotopologues, *J. Phys. Chem. Ref. Data* **46**, 023104 (2017).
- [6] Markó, L., Jákli, G., and Jancsó, G., Vapour pressure of heavy water at its triple point, *J. Chem. Thermodyn.* **21**, 437-441 (1989).

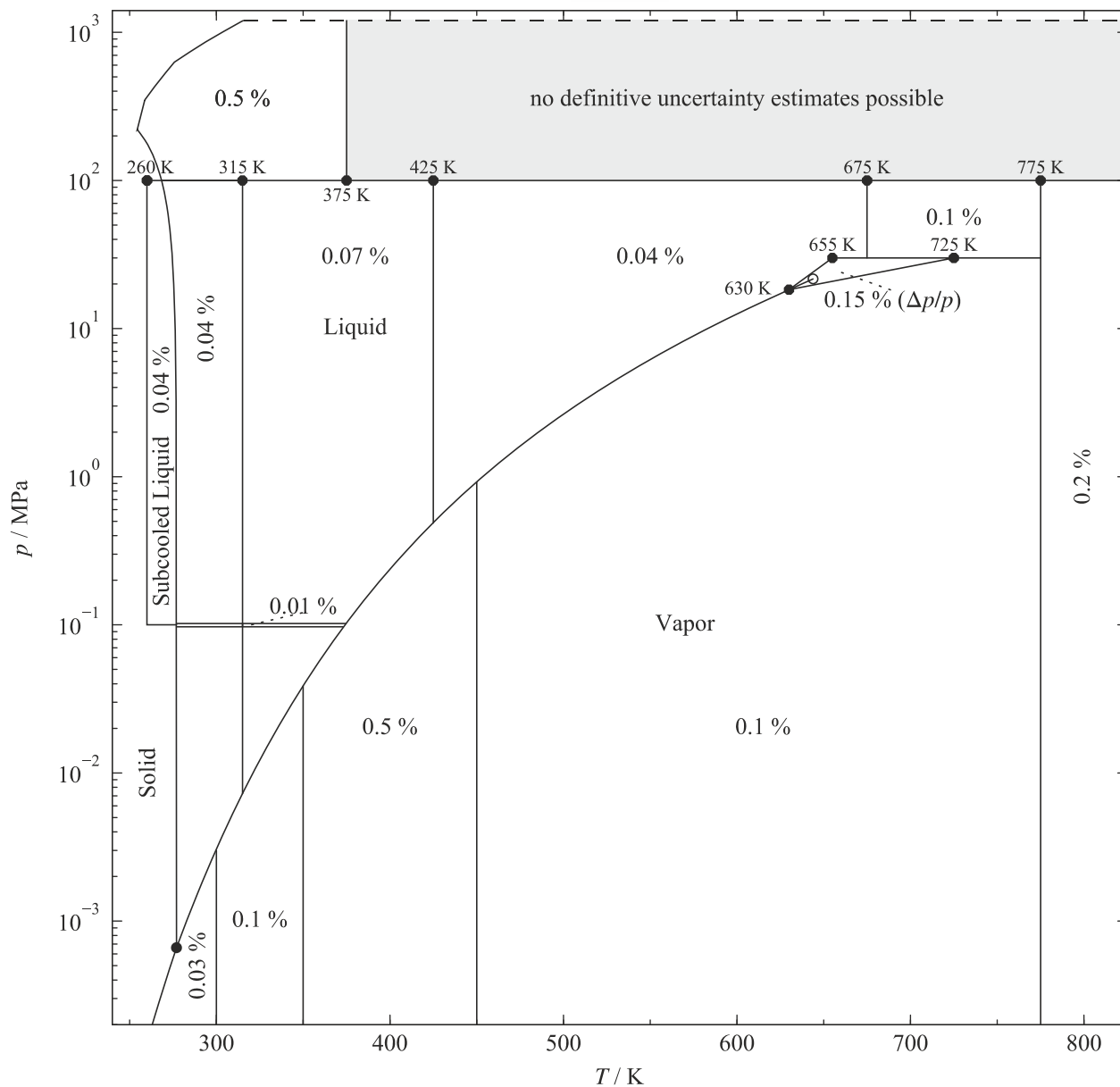


**Fig. 1.** Expanded relative uncertainties in density,  $\Delta\rho/\rho$ , estimated for Eq. (5). In the enlarged critical region (triangle), the uncertainty is given as percentage uncertainty in pressure,  $\Delta p/p$ . This region is bordered by the two isochores  $8 \text{ mol dm}^{-3}$  and  $29 \text{ mol dm}^{-3}$  and by the 30 MPa isobar. The positions of the lines separating the uncertainty regions are approximate. At low pressures for the vapor, the uncertainties become much smaller than indicated because the vapor is nearly an ideal gas.

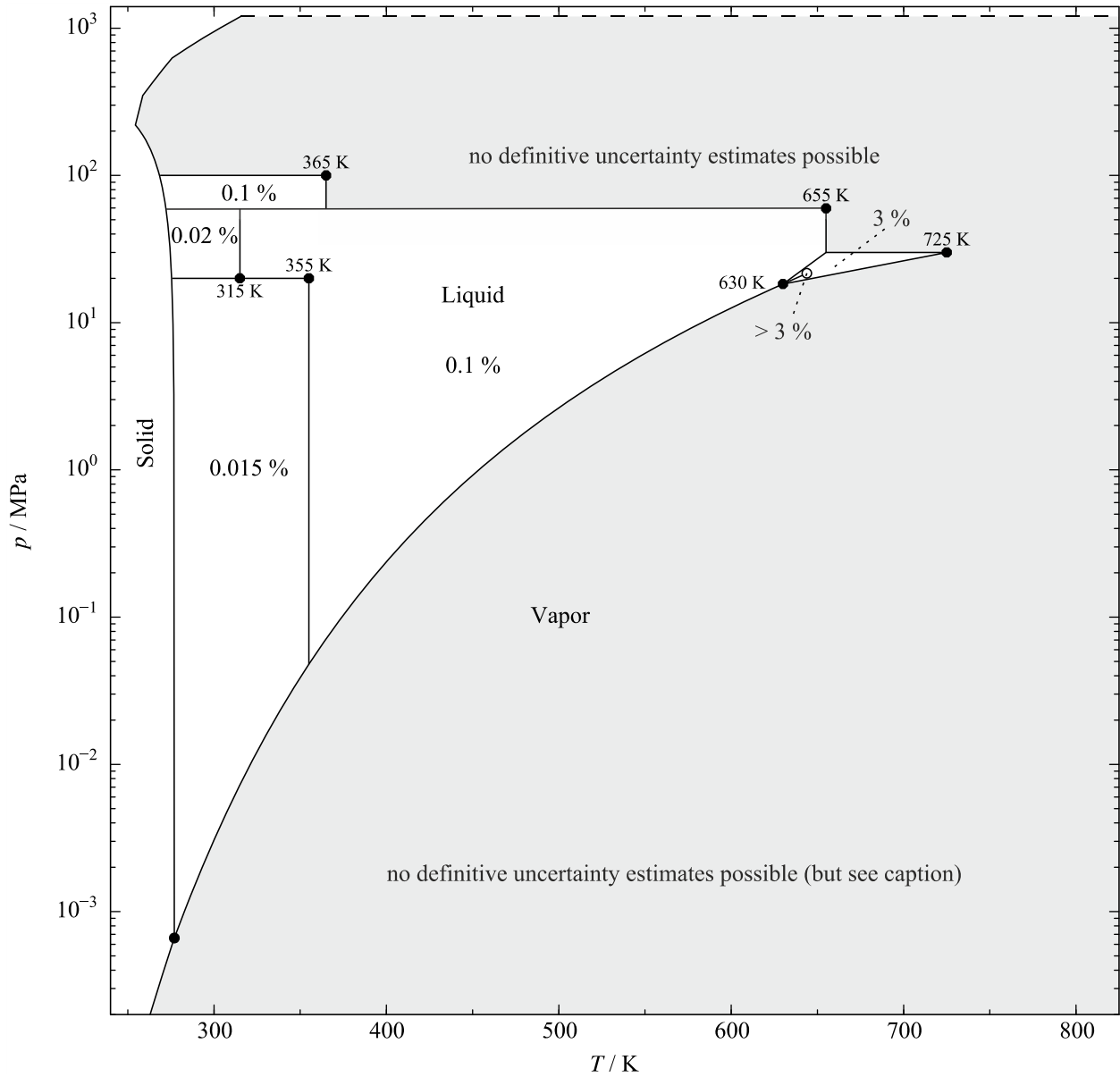


**Fig. 2.** Expanded relative uncertainties in speed of sound,  $\Delta w/w$ , estimated for Eq. (5). For the definition of the triangle around the critical point, see the Fig. 1 caption. The positions of the lines separating the uncertainty regions are approximate. At low pressures for the vapor, the uncertainty becomes small because the vapor approaches the ideal-gas limit.

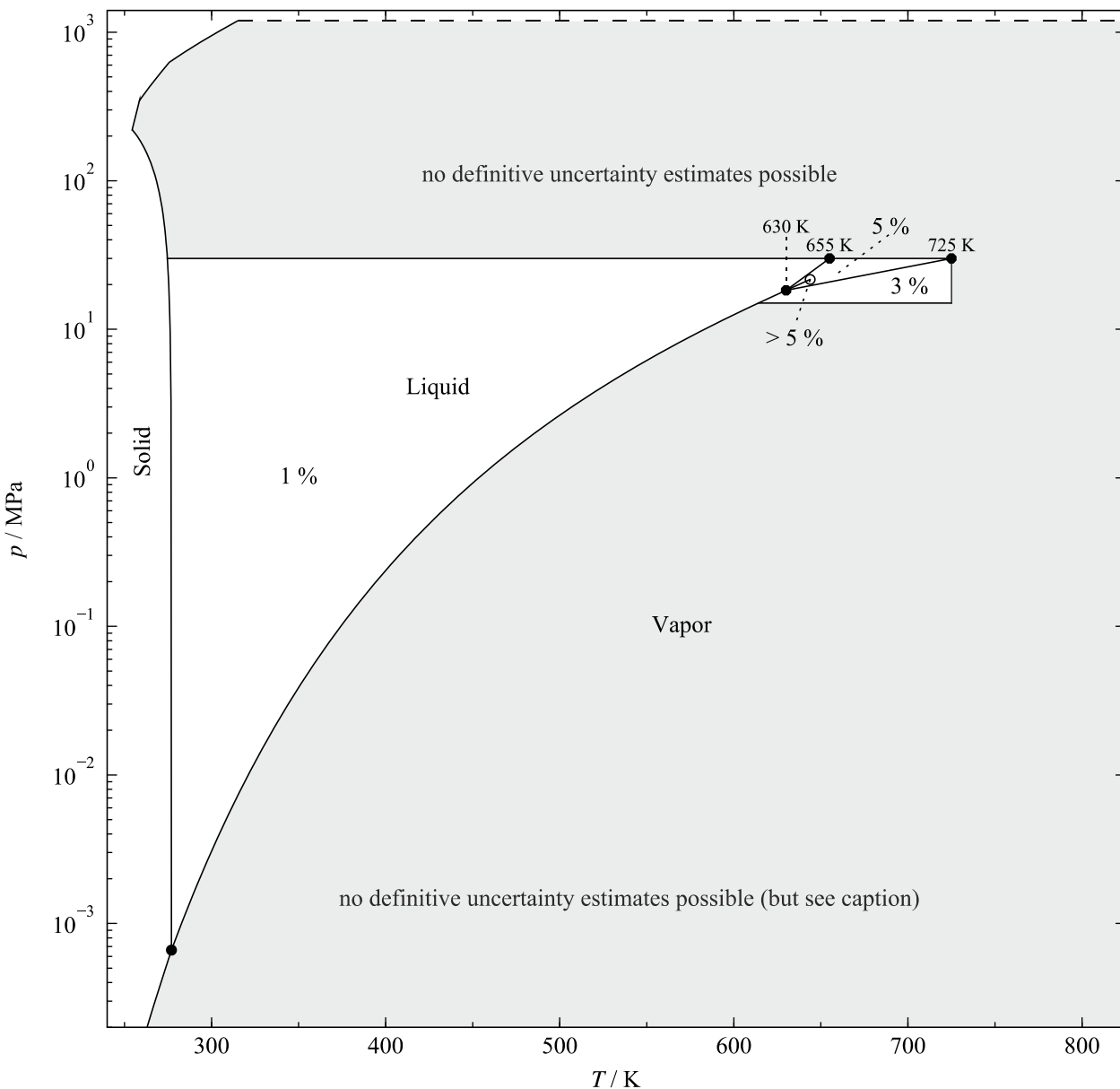


**Fig. 3.** Expanded relative uncertainties in specific isobaric heat capacity,  $\Delta c_p/c_p$ , estimated for Eq. (5). For the definition of the triangle around the critical point, see the Fig. 1 caption. The positions of the lines separating the uncertainty regions are approximate. The uncertainty in the vapor phase at low pressures approaches the uncertainty of the ideal-gas heat capacity, which is less than 0.02 %.

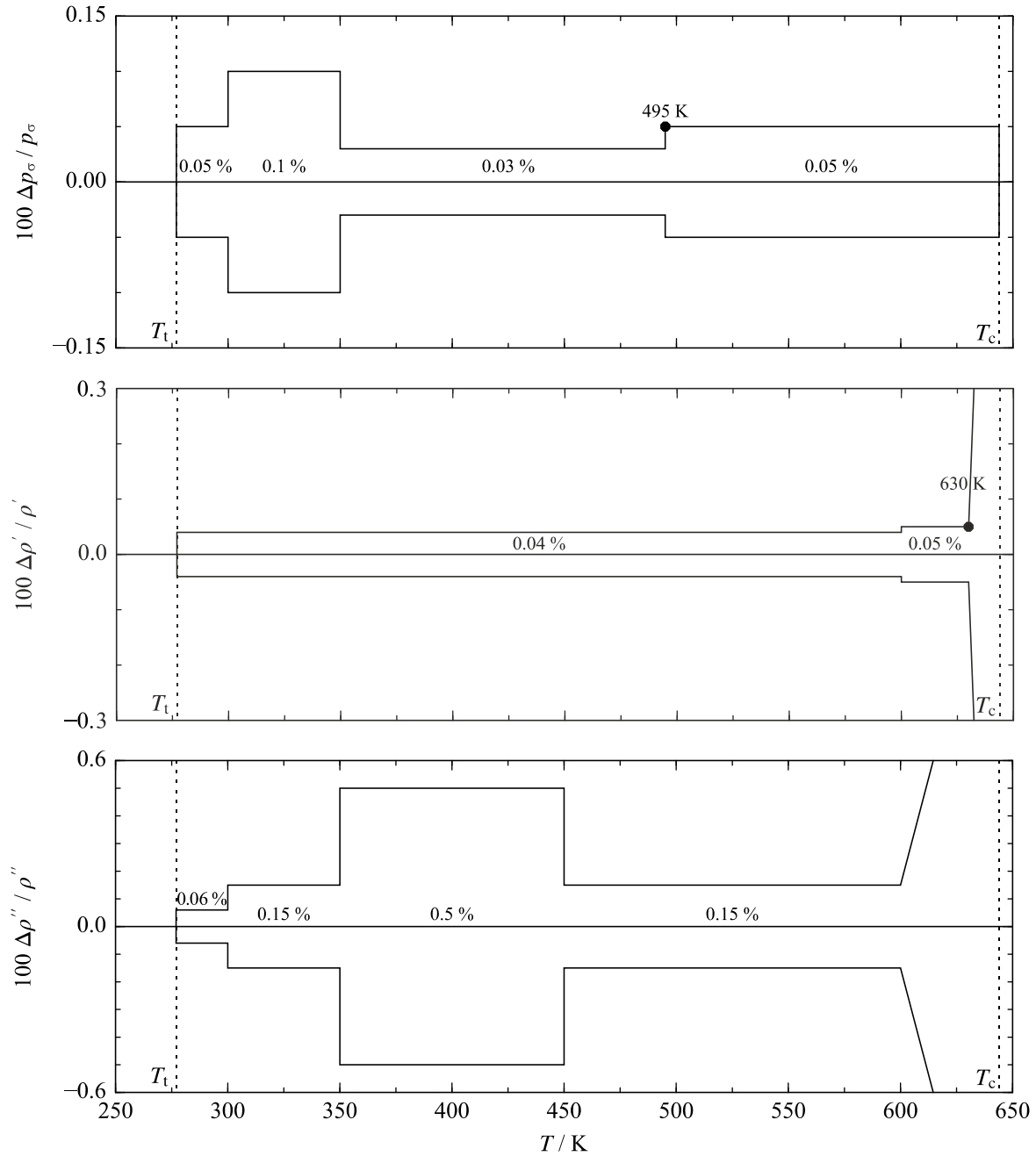


**Fig. 4.** Uncertainties in vapor pressure,  $\Delta p_\sigma / p_\sigma$ , in saturated liquid density,  $\Delta \rho' / \rho'$ , and in saturated vapor density,  $\Delta \rho'' / \rho''$ , estimated for Eq. (5). The uncertainties for the saturated densities increase to 1.5 % at the critical temperature.